THESIS FOR THE DEGREE OF LICENTIATE OF ENGINEERING IN SOLID AND STRUCTURAL MECHANICS

Predicting rolling contact fatigue crack initiation in highly deformed rail steel

NASRIN TALEBI

Department of Industrial and Materials Science
Chalmers University of Technology
Gothenburg, Sweden, 2024

Predicting rolling contact fatigue crack initiation in highly deformed rail steel

NASRIN TALEBI

Thesis for the degree of Licentiate of Engineering
Technical Report No. IMS-2024-12

Department of Industrial and Materials Science
Chalmers University of Technology
SE-412 96 Gothenburg, Sweden
Phone: +46(0)31 772 1000

Cover:
Accumulated damage after one load sequence in a railhead with deformed material

Printed by Chalmers Digitaltryck,
Gothenburg, Sweden 2024.

To maman, baba, Saeed, and Kourosh.

Predicting rolling contact fatigue crack initiation in highly deformed rail steel

NASRIN TALEBI

Department of Industrial and Materials Science
Chalmers University of Technology

Abstract

Rolling Contact Fatigue crack initiation is often associated with large accumulated plastic deformations in the surface layer of rails and wheels. These deformations are known to affect the mechanical and fatigue behavior of the material. Even so, many fatigue crack initiation predictions in literature do not account for the influence of the deformed near-surface material. This thesis focuses on developing modeling methodologies that account for the long-term accumulation of plastic deformations in fatigue crack initiation predictions.

The first part of the thesis deals with evaluating and improving fatigue crack initiation criteria for severely deformed R260 pearlitic steel. This enhancement is addressed by proposing modified criteria. Three groups of experiments form the basis for the evaluations: Axial-torsion tests with large shear strain increments (predeformation), uniaxial or proportional multiaxial low cycle fatigue tests after different amounts of predeformation, and uniaxial high cycle fatigue experiments. To assess the performance of both existing and proposed crack initiation criteria, a cross-validation procedure is used. The proposed criterion, which accounts for the influence of accumulated plastic strains on fatigue crack initiation, improves the fit to the experimental data. Although there is a tendency to overfitting, this can be mitigated by considering more experiments.

In the second part of the thesis, fatigue crack initiation in a railhead subjected to realistic traffic loading is investigated, focusing on the influence of the large accumulated plastic deformations near the surface. The adopted anisotropic material model is calibrated against experiments with railway-like loading at different material states, corresponding to different depths in the railhead. The identified material parameters are then used to consider spatially varying properties in the railhead. This variation is governed by the accumulated shear strain distribution, obtained from measurements in field samples. By using the stresses and strains from finite element simulations of wheel over-rollings, the previously developed crack initiation criterion is applied. The results highlight the importance of considering the deformed near-surface material in a railhead when predicting fatigue crack initiation, as it is shown to reduce fatigue damage growth during a traffic load sequence.

Keywords: Railway mechanics, plasticity, fatigue crack initiation, anisotropy, predeformation, railway-like loading tests, parameter identification, over-rolling simulations

List of Publications

This thesis is based on the following publications:

[**Paper A**] N. Talebi, J. Ahlström, M. Ekh, K. A. Meyer, "Evaluations and enhancements of fatigue crack initiation criteria for steels subjected to large shear deformations," *International Journal of Fatigue,* vol. 182, p. 108 227, 2024.

[**Paper B**] N. Talebi, B. Andersson, M. Ekh, K. A. Meyer "Influence of a highly deformed surface layer on RCF predictions for rails in service," *To be submitted for international publication.*

The appended papers were prepared in collaboration with the co-authors. The author of this thesis was responsible for the major progress of the work, including taking part in the planning of the papers, developing theoretical and computational frameworks, developing the numerical implementations, running the simulations, and writing the papers.

Publication by the author, not included in this thesis, is:

N. Talebi, J. Ahlström, M. Ekh, K. A. Meyer, "Crack initiation criteria for deformed anisotropic R260 rail steel," *CM 2022 - 12th International Conference on Contact Mechanics and Wear of Rail/Wheel Systems, Conference Proceedings,* pp. 857–864, 2022.

Preface and Acknowledgment

The work presented in this thesis was carried out at the Department of Industrial and Materials Science at Chalmers University of Technology within the research project MU41 "Crack initiation in anisotropic wheel/rail material." This project has been part of the ongoing research activities within the National Center of Excellence CHARMEC (CHAlmers Railway MEChanics). This study is partially funded within the European Union's Horizon 2020 research and innovation program in the Shift2Rail project In2Track3 under grant agreement number 101012456 and in Europe's Rail project IAM4RAIL under grant agreement number 101101966. In particular, the support from Trafikverket and voestalpine Railway Systems GmbH is gratefully acknowledged. The majority of the numerical simulations in this thesis were enabled by resources provided by the National Academic Infrastructure for Supercomputing in Sweden (NAISS) at Chalmers Center for Computational Science and Engineering (C3SE) partially funded by the Swedish Research Council through a grant agreement number 2022-06725.

I would like to express my gratitude to my main supervisor, Prof. Magnus Ekh, for your endless support, guidance, and encouragement throughout my research work. I am grateful for being given the opportunity to work with you and learn from you. You provide a work environment that makes research more enjoyable! I would like to thank my co-supervisors, Prof. Johan Ahlström and Dr. Knut Andreas Meyer. Thank you, Johan, for your generous support and for being so kind to me. Thank you, Knut, for always being available and welcoming for our meetings and discussions. I look forward to working more closely together at Chalmers!

I would like to extend my appreciation to the CHARMEC group and our research partners for your insightful input and valuable discussions during our workshops and reference group meetings. I would like to say a special thanks to my co-author, Björn Andersson, for helping me with the wheel over-rolling simulations patiently!

Also, I want to thank all my friends and colleagues at the Division of Material and Computational Mechanics and at the Division of Dynamics for creating a welcoming and friendly work environment. The work would not be as enjoyable without you!

Also, I would like to thank my family for your unconditional love and sacrifices. Thank you, my brother Saeed, for always being there for me. Last but certainly not least, I would like to express my deepest gratitude to my husband, Kourosh. Your presence by my side, belief in me, selfless love, and infinite support have been my greatest motivation throughout this way!

Gothenburg, August 2024,
Nasrin Talebi

Contents

Part I

Extended Summary

CHAPTER 1

Introduction

In this chapter, the background and motivation for this work, along with the research objectives and scope, are presented.

1.1 Background and motivation

Repeated loading from wheels rolling over the rail causes Rolling Contact Fatigue (RCF), which is recognized as a major source of problems in the railway industry [1], [2]. Wheel-rail contact generates high contact pressure, as well as large shear stresses due to tractive and cornering forces, on the surfaces of rails and wheels, resulting in severe plastic deformations [3], [4], see Figure 1.1(b). Accumulation of the large plastic deformations in the near-surface material during service induces anisotropic material behavior [5]. These high deformations are known to be the source for the initiation of common RCF defects, such as gauge corner cracks, shown in Figure 1.1(a), cf. [6], [7]. RCF defects reduce the reliability and safety of railways, and the mitigation costs

(a) (b)

Figure 1.1: (a) Gauge corner cracks (Photo: Anders Ekberg), and (b) the deformed surface layer at the gauge corner of a rail (45° to the longitudinal direction) [8]

are very high. For instance, the annual cost in the European rail system was estimated to be 300 MEUR in the year 2000 [1]. Understanding the mechanical and fatigue behavior of the heavily deformed and anisotropic material can assist railway manufacturers and infrastructure managers in enhancing manufacturing and maintenance planning, reducing RCF-related costs.

Investigating the fatigue behavior of the anisotropic near-surface material is a complicated problem. This thesis focuses on studying how fatigue crack initiation is affected by the deformation-induced anisotropy in the near-surface material under pure mechanical loading. RCF crack propagation is the topic of other related CHARMEC projects (MU35, MU38). To address fatigue crack initiation, it is essential to develop a modeling procedure that includes constitutive models describing the complex near-surface material behavior, efficient and accurate Finite Element (FE) simulations of wheel-rail contact, and fatigue crack initiation criteria accounting for the deformed material behavior. Much work has been performed on the first two areas in the previous CHARMEC projects (MU14, MU19, MU34, MU37), and the third one is the primary objective of this thesis. However, these models need to be calibrated and validated against experimental data with respect to long-term cyclic and multiaxial loading to accurately predict RCF cracks in real-world conditions. Due to the large gradient of properties in the highly deformed surface layer, characterizing material behavior using standard testing methods is very difficult. Therefore, this thesis uses experimental data from the special technique developed in the CHARMEC project MU34 to calibrate and validate the adopted and developed models.

1.2 Aim of research

The ultimate goal of this research study is to enrich the understanding of the influence of long-term accumulation of plastic deformations on the fatigue crack initiation performance of R260 pearlitic steel through improvement of material models and fatigue crack initiation criteria. To this end, the following parts are completed and presented in this thesis:

- evaluation and further development of fatigue crack initiation criteria for severely shear-deformed steels (**Paper A**)

- simulation-based investigation of the impact of highly deformed near-surface material in rails under in-service loading on fatigue crack initiation (**Paper B**)

The following future parts are foreseen in the second part of the project:

- consider a railhead with deformed geometry in the over-rolling simulations of **Paper B**

- substitute a standard cyclic plasticity model with a cycle-domain model

- employ the cycle-domain model to simulate the whole life of a railhead under realistic traffic loading (from virgin to highly deformed material states)
- validate the predictions of RCF crack initiation against field measurements

1.3 Scope of research

The main focus of this thesis is to predict the initiation of macroscopic RCF cracks in highly deformed surface layer of rails under pure mechanical loading. Studying the subsequent propagation of the macroscopic cracks is dealt with in other related CHARMEC projects. Conducting experiments is out of the scope of this thesis. We study R260 pearlitic rail steel primarily, but the adopted and developed approaches can also be relevant to studying wheel materials. Investigating the influence of thermal loading, employing coupled continuum damage models, as well as integrating crack initiation and propagation modeling efforts, can be considered as future extensions of this work.

CHAPTER 2

Considered experiments

This chapter describes the considered experiments in the thesis, namely predeformation, Low Cycle Fatigue (LCF), and High Cycle Fatigue (HCF) tests. These experiments provide data for calibration and validation of the adopted and developed models. The predeformation tests mimic the severely deformed material near the surface of rails, as well as the loading condition experienced by a rail in service. The LCF and HCF tests are further used to calibrate the employed and proposed models for anisotropic material with respect to long-term cyclic and multiaxial loading. The field samples extracted from the main railway line in Sweden, between Stockholm and Gothenburg, formed the basis for evaluating the predeformation technique in [8]. In this line, traffic is dominated by passenger trains with axle loads between 15-19 tons. The annual traffic is in the order of $15 \cdot 10^6$ tones, resulting in about 10^6 wheel passages.

2.1 Predeformation

As previously mentioned, due to large strain gradients in the surface layer of rails, conducting conventional experiments on the material of this layer to understand its mechanical behavior is very difficult. Equal angular channel pressing and high pressure torsion have been used previously in literature to replicate the material state found in the surface layer of rails [9]–[12]. However, a limitation of these methods is that the extracted samples are very small, making it difficult to achieve axisymmetric specimens needed for multiaxial fatigue testing. Meyer et al. [8] developed an experimental technique using axisymmetric test bars in an axial-torsion machine in order to mimic the accumulation of shear strains in the surface layer of rails. In this technique, a test bar is twisted in steps of 90° under a constant axial load. A test bar before and after predeformation is shown in Figure 2.1(a), where the laser-etched lines visualize the surface shear strains. The loading condition in these experiments, i.e., combined shear and tension-compression, is similar to that experienced by rail steel during wheel-rail rolling contact [13], and cracks were observed on the test bars' surfaces. These facts motivate using the experimental results to investigate the fatigue behavior of the deformed material representing the

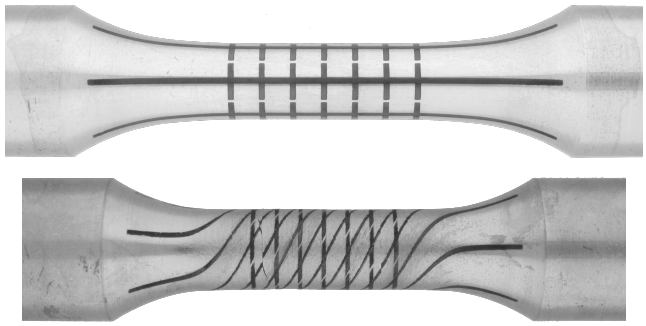

(a)

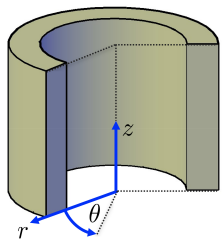

(b)

Figure 2.1: (a) Undeformed (top) and predeformed (bottom) test bar [8], and (b) definition of cylindrical coordinate system in the thin-walled tubular test bars.

material at a certain depth of a rail, see **Paper A**.

2.2 Multiaxial low cycle fatigue

Due to the low number of cycles to failure in the predeformation tests, previously conducted LCF experiments are also included in the evaluations of fatigue crack initiation criteria in **Paper A**. In these tests, the predeformed solid test bars were remachined into thin-walled tubular shapes and were subjected to pure axial, pure shear, or proportional multiaxial loading [14]. Most of the fatigue life was spent on macroscopic crack initiation, and the crack propagation regime was negligible (less than 1.1% of the total life).

In **Paper B**, in addition to the pure axial and pure shear test results, data from multiaxial LCF experiments under non-proportional loading (compression and shear), preceded by different amounts of predeformation, are also considered. These data are employed to calibrate the adopted plasticity model described in Section 3.2. The purpose of these experiments is to subject rail steel to pulsating compression and alternating shear, replicating the in-service wheel-rail rolling contact loading [15]. In the non-proportional loading experiments, a

test bar is first subjected to compressive normal strain ϵ_{zz} and shear strain $\gamma_{z\theta}$ in a specific loading direction (see Figure 2.1(b) for the definition of coordinate system). The shear strain, $\gamma_{z\theta}$, gradually reverses to an equal magnitude in the opposite direction, while ϵ_{zz} is held constant. The loading cycle ends when both strains are reduced to zero. In both proportional and non-proportional loading experiments, the equivalent von Mises strain amplitude was 0.8% on the test bars' surfaces. Some results from the non-proportional loading tests are illustrated in Figure 2.2. An important observation in Figures 2.2(a) and 2.2(c) for cycle 1 is that, hardening increases with higher levels of predeformation, which is particularly pronounced when comparing PD_0 and PD_1. A similar trend can be observed when considering the axial and shear stress-strain response in cycle 500 in Figures 2.2(b) and 2.2(d). Further, after 500 cycles, material softening becomes apparent, especially in the axial response, see Figure 2.2(b).

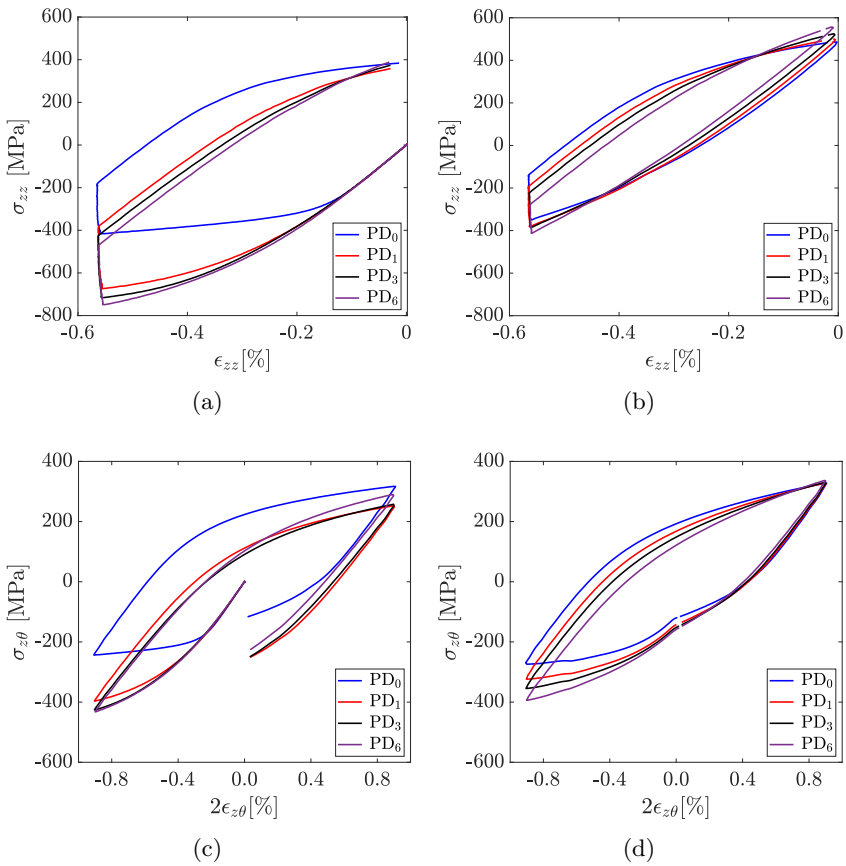

Figure 2.2: Axial stress-strain response for (a) cycle 1 and (b) cycle 500, shear stress-strain response for (c) cycle 1 and (d) cycle 500, from experiments. Note that, PD_x refers to x cycles of predeformation.

2.3 Uniaxial high cycle fatigue

In **Paper A**, we use the results from the axial HCF experiments conducted by Christodoulou et al. [16] on pearlitic rail steel Grade 900 A, as one part of calibration data. The aim is to account for both HCF and LCF regimes in the Jiang-Sehitoglu and the modified criteria, see Section 3.5. In [16], based on the derived S-N curve shown in Figure 2.3, the fatigue limit was determined to be 540 MPa at a fatigue life of 10^7 cycles. We use the fatigue limit and the stress ratio of 0.1 from these experiments in the calibration procedure, see Section 3.5.

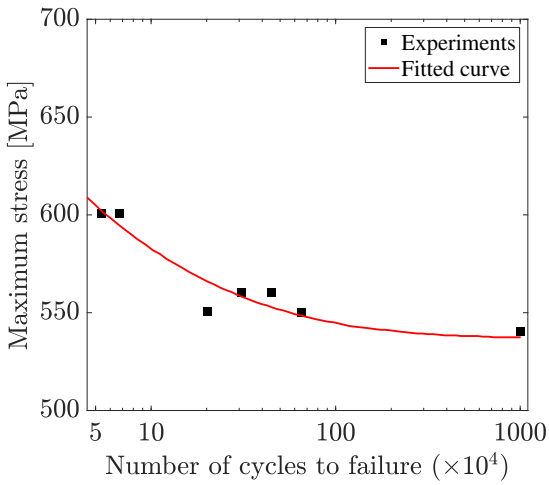

Figure 2.3: Fatigue S-N curve, data from [16].

CHAPTER 3

Modeling

Describing the behavior of rail material that has undergone significant plastic deformations, leading to heterogeneous material properties, is the modeling challenge in this thesis. This chapter presents the adopted and developed modeling strategies and tools to deal with the challenge.

3.1 Distribution of accumulated shear strain

As previously mentioned, during wheel-rail rolling contact, severe plastic shear strains accumulate, even during the early loading cycles. In **Paper B**, we use the measured accumulated shear strains versus depth at two locations in the railhead, points P_2 and P_3 in Figure 3.1, from [8]. Based on the typical contact regions, we assume that the accumulated shear strains are zero outside points P_1 and P_4. Moreover, the depth of the anisotropic layer is assumed to be 0.5 mm, and outside this depth, the material is considered isotropic. We propose to linearly interpolate between the distributions at the points P_2 and P_3, together with zero shear strains at any depth at the points P_1 and P_4, in the introduced $\xi - \eta$ coordinate system. Figure 3.1 illustrates the distribution of the accumulated shear strain, γ, in the railhead cross-section of a 50E3 rail profile, where γ decreases in depth and also varies in the transverse direction. In the wheel over-rolling simulations (see Section 3.4), we use the distribution of γ to define a railhead cross-section with deformed near-surface material, whose properties vary depending on the given spatial position. Moreover, the initiation of fatigue cracks is influenced by the γ-dependent initial ratcheting strains in the railhead, see Section 3.5.

3.2 Material model

Reliable predictions of crack initiation require accurate approximations of stress and strain histories in the material. However, the large plastic deformations in the rail result in complex material behavior, necessitating the use of finite strain plasticity models with advanced hardening laws and anisotropic yield surfaces. In **Paper A**, we adopt such a model [17] to obtain accurate stresses

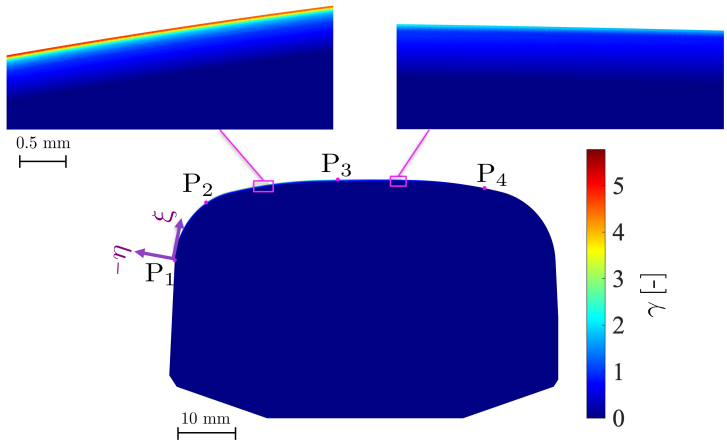

Figure 3.1: Assumed distribution of the accumulated shear strain, γ, over the railhead cross-section.

and strains during the predeformation experiments. Distortional hardening is accounted for through the evolving anisotropy tensor $\hat{\mathbf{C}}$ in the yield criterion formulated as in [17]

$$\Phi = \sqrt{\boldsymbol{M}_{\text{red}}^{\text{dev}} : \hat{\mathbf{C}} : \boldsymbol{M}_{\text{red}}^{\text{dev}}} - Y \leq 0 \tag{3.1}$$

where $\boldsymbol{M}_{\text{red}}^{\text{dev}}$ is the reduced deviatoric Mandel stress, and Y is the isotropic hardening.

In **Paper B**, we reformulate the advanced material model in [17] in the small-strain framework in order to make it more computationally efficient for use in the wheel over-rolling simulations. We assume that there is no evolution of the anisotropy tensor, $\hat{\mathbf{C}}$, from its initial state, which is described by the accumulated shear strain, γ. Furthermore, we calibrate the material model against the non-proportional multiaxial cyclic tests with railway-like loading (described in Section 2.2) at different predeformation levels. The identified material parameters and anisotropy tensors for each predeformation level are used to consider unique material parameter values at each integration point in the railhead. This spatial variation of material properties is governed by the accumulated shear strain distribution, see Section 3.4.

3.3 2D axisymmetric simulations of predeformations

The shear strains vary radially during predeformation experiments, resulting in an inhomogeneous stress field, such that only the axial force, the specimen's elongation, torque, and twist could be measured, see [8]. Accordingly, in **Paper A** and **Paper B**, 2D FE simulations of the predeformation tests

and the predeformation parts of the LCF tests (described in Chapter 2), are performed in Abaqus [18] to obtain local stress and strain histories, as well as the anisotropy tensor, $\hat{\mathbf{C}}$, for each predeformation level. For these simulations, 8-node quadratic axisymmetric elements with out-of-plane twist (referred to as CGAX8R in Abaqus) and the finite strain model formulation from [17] are employed. Figure 3.2 shows the shear stresses before unloading in the 6^{th} predeformation cycle under nominal compressive stress of -600 MPa, where there is an increase in the shear stress, $\sigma_{z\theta}$, in the radial direction, from the center to the surface of the test bar. In **Paper A**, the extracted local stresses and strains are used as an input to the crack initiation criteria. Moreover, in **Paper B**, the obtained anisotropy tensors from these FE simulations, are used to introduce the deformed material state in the railhead.

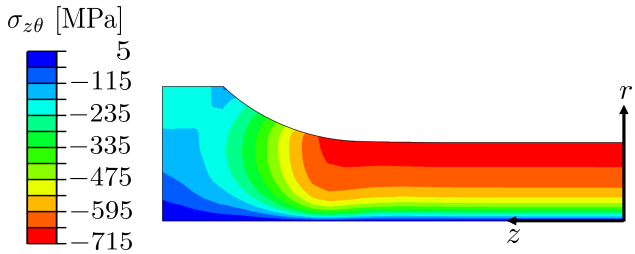

Figure 3.2: Shear stresses in the 6^{th} predeformation cycle, before unloading, at the nominal compressive stress of -600 MPa

3.4 Wheel over-rolling simulations

Due to the challenges of conducting field measurements, such as high costs, time constraints, and the influence of environmental factors, FE simulations of wheel-rail contact have been widely used. These simulations are employed to investigate different phenomena, such as RCF crack initiation [19]–[22], RCF crack propagation [23], [24], and ratcheting behavior [15]. Some recent studies have developed computationally efficient 3D FE approaches, aiming to capture the complexity of rolling contact conditions with lower computational costs [25]–[27]. Despite these improvements, 3D models are still unable to consider many loading cycles while accurately resolving contact regions. To address this limitation, 2D FE models have been developed to reduce the computational time while maintaining reasonable accuracy. These models have been used to investigate, for instance, wear and fatigue crack initiation in rough wheel-rail contact surfaces [28], or to simulate detailed repair welding process [29].

Resolving the large shear strain gradient close to the rail surface in **Paper B** requires a very fine mesh. Therefore, for modeling the rail during train wheel over-rollings, we adopt the 2D Generalized Plane Strain (GPS) model developed by Andersson et al. [29]. In the GPS model, a 2D cross-section is positioned

between two rigid bounding planes which can translate along the longitudinal direction of the rail and rotate around the in-plane axes with respect to a reference point. The translation and rotation of these bounding planes are constrained by assigning axial and bending stiffnesses to the corresponding degrees of freedom. To mimic a Hertzian contact pressure distribution moving longitudinally on the rail surface, the element thicknesses are scaled such that the maximum von Mises stresses in the 2D FE simulations match those from full-scale 3D over-rolling simulations [30].

The representative traffic loading is obtained from the multibody dynamics simulations in [31] of a circular curve, located at the west mainline in Sweden between Nyckelsjön and Sparreholmen. The load sequence consists of 483 wheel passages, representing 20 passenger trains with axle loads ranging from 11.7 to 21.0 tons, different measured wheel profile geometries, and varying vehicle speeds [31].

The over-rolling simulations in **Paper B** consider both homogeneous virgin (isotropic) and inhomogeneously deformed (anisotropic) material states. To account for the deformed material state, we linearly interpolate between the anisotropy tensors and the identified material parameters for each predeformation level. This interpolation is based on the distribution of the accumulated shear strains, see Section 3.1. The resulting distribution of maximum von Mises stress, as well as per-sequence accumulated plasticity and fatigue damage increment from the over-rolling simulations, are presented and discussed in **Paper B**.

In Figure 3.3, the von Mises stress field for both materials during the load cycle with maximum contact pressure and traction is presented. As can be seen, the maximum von Mises stress occurs in the railhead cross-section with deformed and hardened material, and the location is at the surface near the top of the rail where wheel-rail contact takes place. Further details underscoring the importance of considering the deformed near-surface material in RCF crack initiation predictions are provided in **Paper B**.

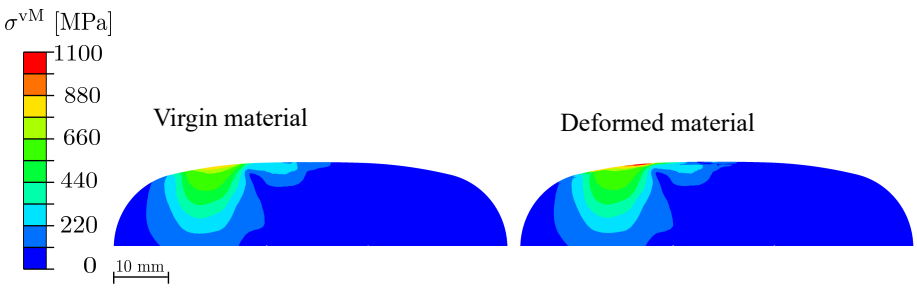

Figure 3.3: Comparison of von Mises stresses in the railhead cross-section for virgin and deformed materials during the load cycle with maximum contact pressure and traction.

3.5 Crack initiation criteria

Predicting fatigue crack initiation is of great importance in railway engineering, as it can be used as an aid when developing methods to delay the initiation of RCF cracks, thereby extending the service life. Many studies have been performed in the area of crack initiation predictions, see e.g. Sadeghi et al. [32] and Ringsberg et al. [33] for reviews. An equivalent plastic strain model proposed by Kapoor [34], a purely energy-density based criterion developed by Golos and Ellyin [35], and approaches taking into account the material microstructure in the fatigue damage predictions [36]–[38] are some of the established criteria and methodologies in literature for crack initiation predictions. Some criteria employ a critical plane search approach to identify the plane experiencing the largest fatigue damage [39]–[42]. Jiang and Sehitoglu [43] suggested that fatigue damage evolution on a given plane is influenced by normal and shear stress and strain ranges.

In [44], it is shown that a more advanced criterion than the Kapoor criterion is required to obtain a reasonable agreement between the predeformation experiments and the corresponding simulation data. Furthermore, in **Paper A** [45], we show that, due to the protective effect of predeformation, the so-called mixed criterion [43], combining the Jiang-Sehitoglu (J-S) and Kapoor criterion, does not lead to significant enhancement. Therefore, we propose and evaluate two modifications to the J-S criterion in order to improve its fitting and predictive abilities. The most successful modification allows the fatigue damage threshold to depend on ratcheting strain as

$$\widetilde{FP}_0\left(\epsilon_\mathrm{r}\right) = FP_\infty - \left(FP_\infty - FP_0\right)\exp\left(\frac{-\epsilon_\mathrm{r}}{\kappa}\right) \tag{3.2}$$

Thereby, the cyclic fatigue damage growth is computed as

$$\frac{\mathrm{d}D_{\mathrm{f},i}}{\mathrm{d}N} = \left(\frac{\left\langle \max_{\boldsymbol{n}} FP - \widetilde{FP}_0 \right\rangle}{C_0}\right)^m \tag{3.3}$$

where the fatigue driving force, FP, on a given plane is quantified as in [43]

$$FP = \frac{\Delta\epsilon}{2}\,\sigma_{\max} + J\,\Delta\gamma\,\Delta\tau \tag{3.4}$$

The idea behind the suggested modifications is to account for an increased resistance against fatigue crack initiation induced by predeformation. This is inspired by the results from the study conducted by Gren and Ahlström [46]. For the railhead with deformed material in the over-rolling simulations, the initial ratcheting strain, ϵ_r, at each integration point is obtained using the simulation results from the predeformation tests and the distribution of accumulated shear strains. The fatigue parameters, m, C_0, J, FP_∞, and κ, are calibrated against the predeformation experiments and proportional multiaxial LCF tests, explained in Chapter 2. Considering the HCF test results (see Section 2.3) and

assuming an elastic material response in the HCF regime, we determine the fatigue parameter, FP_0, by using the normal loading term in Equation 3.4. For further details on the notations, the reader is referred to **Paper A**.

CHAPTER 4

Parameter identification

Connecting advanced models and experimental data through parameter identification forms one important part of the work carried out in this thesis. In **Paper A**, the fatigue parameters of the crack initiation criteria and, in **Paper B**, the material parameters of the adopted plasticity model have been identified using numerical optimization. This chapter presents a brief discussion of the methods used in the appended papers for parameter identification.

4.1 Optimization procedure

A general optimization problem is to find an optimal solution $\boldsymbol{x}_{\text{opt}}$ that minimizes an objective function $f(\boldsymbol{x})$

$$\begin{aligned} \boldsymbol{x}_{\text{opt}} := &\arg \text{ minimum } f(\boldsymbol{x}) \\ &\boldsymbol{x} \in S \end{aligned} \tag{4.1}$$

where $S \subseteq \mathbb{R}^n$ is a nonempty set, $\boldsymbol{x} \in \mathbb{R}^n$ is a vector of model parameters, x_j, $j = 1, ..., n$, and $f : \mathbb{R}^n \to \mathbb{R} \cup \{\pm\infty\}$. Techniques for solving an optimization problem can be divided into two groups: Derivative-free methods, such as Nelder-Mead simplex algorithm [47], [48] or BOBYQA [49], and gradient-based methods, including steepest descent, Newton's method, or Levenberg-Marquardt [50]. Using the Nelder-Mead simplex algorithm with multiple initial guesses has proven successful in previous works, see e.g. [51], [52], and it is thus also adopted in the appended papers. The algorithm is employed to minimize the objective function of a least-square type, which, in general, is formulated as

$$f(\boldsymbol{x}) = \left|\left| \boldsymbol{y}^{\text{exp}} - \boldsymbol{y}^{\text{sim}}(\boldsymbol{x}) \right|\right| \tag{4.2}$$

where $\boldsymbol{y}^{\text{exp}}$ are experimental data, and $\boldsymbol{y}^{\text{sim}}(\boldsymbol{x})$ are the simulated data from the model (as a function of the model parameters, $\boldsymbol{x}$). The general procedure for parameter identification in this thesis is summarized below:

1. specify permissible intervals $\boldsymbol{x}_{\min}$ and $\boldsymbol{x}_{\max}$ for the parameters $\boldsymbol{x}$ and define the parameter space $\Omega = \{\boldsymbol{x} \,|\, \boldsymbol{x}_{\min} \leq \boldsymbol{x} \leq \boldsymbol{x}_{\max}\}$

2. use Latin Hypercube sampling to generate a full set $\mathrm{S}_{\mathrm{full}}$ of initial guesses $\boldsymbol{x}$ within the parameter space Ω

3. use $\mathrm{S}_{\mathrm{full}}$ in **Paper A**, while in **Paper B**, after evaluating the objective function for initial guesses $\boldsymbol{x}$, choose the best $\boldsymbol{x} \in \mathrm{S}_{\mathrm{red}}$ (reduced set), to start optimization from

4. perform optimizations to minimize the objective function $f(\boldsymbol{x})$ for the initial guesses

5. select the k best-optimized parameter sets with the lowest objective function value, resulting in the updated set S_{full}. Pass these as initial guesses (updated $\boldsymbol{x}$) to the subsequent optimization step

6. reduce k

7. repeat the steps 4 to 6 until convergence

More details of the optimization procedure are explained in **Papers A** and **B**. In **Paper A**, the objective function minimizes the difference between the fatigue crack initiation lives from the experiments and simulations. Since the magnitudes of the fatigue lives observed in the experiments are significantly different, the contributions to the objective function are normalized by the corresponding experimental values. The fatigue parameters, as well as the plasticity model parameters in **Paper B**, are normalized, ensuring that the objective function's sensitivity to small perturbations in the values of the parameters is approximately equal. An observed issue with the Nelder-Mead simplex algorithm was its tendency to stick to the lower or upper bounds of the parameters. To mitigate this problem and improve the robustness of the optimization procedure, it is important to be liberal with the size of the permissible intervals.

As was observed in the experimental results in Figure 2.2, the stress-strain response varies between different levels of predeformation. Hence, in **Paper B**, we identify the 14 material parameters of the adopted plasticity model based on the experiments at each predeformation level. Particularly, we use certain experiments to identify specific material parameters, thereby reducing the complexity of the optimization procedure, see e.g. [53]. Young's modulus E and shear modulus G are determined based on the mean values of the elastic moduli during the pure axial and pure shear loading experiments, respectively (no optimization has been performed). The initial back-stress is optimized against the monotonic parts of the first loading cycles from four uniaxial LCF experiments with different loading directions. The remaining material parameters have been identified in a step-wise approach. In summary, a set of optimized parameters with the lowest objective function values are chosen as the starting points for the subsequent optimization step. The reason behind using this procedure is to guide the optimization algorithm towards finding the optimal solution.

4.2 Prediction and cross-validation

The quality of a model cannot be evaluated only by its ability to fit experimental data, as considering more independent model parameters may improve the fit but reduce the model predictive ability (i.e. overfitting). Accordingly, in **Paper A**, a one-fold cross-validation [54] is employed to assess the performance of each crack initiation criterion on new data and to mitigate the risk of overfitting. This method involves dividing the experimental dataset (with size p) into calibration data (with size $p-1$) and validation data (with size 1) in p possible ways. In **Paper B**, some experimental data are retained to evaluate the predictive ability of the plasticity model.

CHAPTER 5

Summary of appended papers

Paper A

N. Talebi, J. Ahlström, M. Ekh, K. A. Meyer, "Evaluations and enhancements of fatigue crack initiation criteria for steels subjected to large shear deformations," *International Journal of Fatigue,* vol. 182, p. 108 227, 2024.

In this paper, we evaluate the performance of commonly used crack initiation criteria in railway engineering for predicting experimental results of heavily deformed R260 pearlitic steel. Furthermore, modifications to the crack initiation criteria are suggested. The evaluations are based on three groups of experiments: Combined axial-torsion tests with large shear strain increments (predeformation), proportional multiaxial low cycle fatigue experiments preceded by different levels of predeformation, and uniaxial high cycle fatigue tests. Finite element simulations of the predeformation tests, with a finite-strain plasticity model accounting for isotropic, kinematic, and distortional hardening, provide local stress and strain predictions. A cross-validation approach is adopted to examine the capability and reliability of both existing and proposed criteria. One of the proposed modifications noticeably improves the fitting error while maintaining a similar prediction error. Furthermore, it is also able to fit satisfactorily when all experimental data are included in the optimization, indicating its potential for further improvements with the availability of more experimental data.

Paper B

N. Talebi, B. Andersson, M. Ekh, K. A. Meyer "Influence of a highly deformed surface layer on RCF predictions for rails in service," *To be submitted for international publication.*

The main objective of this paper is to investigate how deformed near-surface material affects the mechanical behavior and fatigue crack initiation of a rail under in-service loading. We consider multiaxial low cycle fatigue experiments

under non-proportional loading at different levels of predeformation, representing the material behavior for different amounts of accumulated shear strains. By calibrating an anisotropic plasticity model against these experiments, we obtain a model that represents material behavior at different spatial positions in the railhead cross-section. This variation is governed by the accumulated shear strain distribution in the railhead, obtained from measured shear strains. We use an efficient FE-simulation setup for modeling two rails subjected to realistic traffic situations: One with virgin and one with inhomogeneously deformed material. The results reveal that, in the railhead with deformed material, the maximum von Mises stresses and per-sequence accumulated plasticity are much higher than those in the railhead with virgin material. Using the proposed crack initiation criterion from **Paper A**, we evaluate the fatigue behavior of both materials, demonstrating that the deformed material noticeably reduces the accumulation rate of fatigue damage. These findings highlight the importance of accounting for the deformed near-surface material in a railhead when predicting fatigue crack initiation.

Bibliography

[1] E. E. Magel, 'Rolling contact fatigue: A comprehensive review,' US Department of Transportation, Federal Railroad Administration, Tech. Rep., 2011, 132 p.

[2] A. Ekberg, B. Åkesson and E. Kabo, 'Wheel/rail rolling contact fatigue – probe, predict, prevent,' *Wear*, vol. 314, pp. 2–12, 2014.

[3] F. A. Alwahdi, A. Kapoor and F. J. Franklin, 'Subsurface microstructural analysis and mechanical properties of pearlitic rail steels in service,' *Wear*, vol. 302, pp. 1453–1460, 2013.

[4] D. Benoît, B. Salima and R. Marion, 'Multiscale characterization of head check initiation on rails under rolling contact fatigue: Mechanical and microstructure analysis,' *Wear*, vol. 366-367, pp. 383–391, 2016.

[5] B. Dylewski, M. Risbet and S. Bouvier, 'The tridimensional gradient of microstructure in worn rails – Experimental characterization of plastic deformation accumulated by RCF,' *Wear*, vol. 392-393, pp. 50–59, 2017.

[6] D. F. Cannon, K. Edel, S. L. Grassie and K. Sawley, 'Rail defects: An overview,' *Fatigue and Fracture of Engineering Materials and Structures*, vol. 26, pp. 865–886, 2003.

[7] D. I. Fletcher, F. J. Franklin and A. Kapoor, 'Rail surface fatigue and wear,' in *Wheel–rail interface handbook,* Elsevier, pp. 280–310, 2009.

[8] K. A. Meyer, D. Nikas and J. Ahlström, 'Microstructure and mechanical properties of the running band in a pearlitic rail steel: Comparison between biaxially deformed steel and field samples,' *Wear*, vol. 396-397, pp. 12–21, 2018.

[9] F. Wetscher, R. Stock and R. Pippan, 'Changes in the mechanical properties of a pearlitic steel due to large shear deformation,' *Materials Science and Engineering A*, vol. 445-446, pp. 237–243, 2007.

[10] A. Hohenwarter, A. Taylor, R. Stock and R. Pippan, 'Effect of large shear deformations on the fracture behavior of a fully pearlitic steel,' *Metallurgical and Materials Transactions A: Physical Metallurgy and Materials Science*, vol. 42, pp. 1609–1618, 2011.

[11] T. Leitner, G. Trummer, R. Pippan and A. Hohenwarter, 'Influence of severe plastic deformation and specimen orientation on the fatigue crack propagation behavior of a pearlitic steel,' *Materials Science and Engineering: A*, vol. 710, pp. 260–270, 2018.

[12] T. Leitner, A. Hohenwarter and R. Pippan, 'Anisotropy in fracture and fatigue resistance of pearlitic steels and its effect on the crack path,' *International Journal of Fatigue*, vol. 124, pp. 528–536, 2019.

[13] L. Reis, B. Li and M. de Freitas, 'A multiaxial fatigue approach to rolling contact fatigue in railways,' *International Journal of Fatigue*, vol. 67, pp. 191–202, 2014.

[14] K. A. Meyer, M. Ekh and J. Ahlström, 'Anisotropic yield surfaces after large shear deformations in pearlitic steel,' *European Journal of Mechanics, A/Solids*, vol. 82, p. 103 977, 2020.

[15] C. L. Pun, Q. Kan, P. J. Mutton, G. Kang and W. Yan, 'Ratcheting behaviour of high strength rail steels under bi-axial compression-torsion loadings: Experiment and simulation,' *International Journal of Fatigue*, vol. 66, pp. 138–154, 2014.

[16] P. I. Christodoulou, A. T. Kermanidis and G. N. Haidemenopoulos, 'Fatigue and fracture behavior of pearlitic Grade 900A steel used in railway applications,' *Theoretical and Applied Fracture Mechanics*, vol. 83, pp. 51–59, 2016.

[17] K. A. Meyer and A. Menzel, 'A distortional hardening model for finite plasticity,' *International Journal of Solids and Structures*, vol. 232, p. 111 055, 2021.

[18] Dassault Systèmes, *Abaqus*, 2020.

[19] J. W. Ringsberg, 'Life prediction of rolling contact fatigue crack initiation,' *International Journal of Fatigue*, vol. 23, pp. 575–586, 2001.

[20] E. Kabo, A. Ekberg, P. T. Torstensson and T. Vernersson, 'Rolling contact fatigue prediction for rails and comparisons with test rig results,' *Proceedings of the Institution of Mechanical Engineers, Part F: Journal of Rail and Rapid Transit*, vol. 224, pp. 303–317, 2010.

[21] G. Trummer, C. Marte, P. Dietmaier, C. Sommitsch and K. Six, 'Modeling surface rolling contact fatigue crack initiation taking severe plastic shear deformation into account,' *Wear*, vol. 352, pp. 136–145, 2016.

[22] M. Ghodrati, M. Ahmadian and R. Mirzaeifar, 'Three-dimensional study of rolling contact fatigue using crystal plasticity and cohesive zone method,' *International Journal of Fatigue*, vol. 128, p. 105 208, 2019.

[23] J. Brouzoulis and M. Ekh, 'Crack propagation in rails under rolling contact fatigue loading conditions based on material forces,' *International Journal of Fatigue*, vol. 45, pp. 98–105, 2012.

[24] M. Salahi, F. Larsson, E. Kabo and A. Ekberg, 'Numerical prediction of railhead rolling contact fatigue crack growth,' *Wear*, vol. 530–531, p. 205 003, 2023.

[25] K. A. Meyer, R. Skrypnyk and M. Pletz, 'Efficient 3d finite element modeling of cyclic elasto-plastic rolling contact,' *Tribology International*, vol. 161, p. 107 053, 2021.

[26] F. Ren, Z. Yang and Z. Li, 'An efficient 3D finite element procedure for simulating wheel–rail cyclic contact and ratcheting,' *Tribology International*, vol. 198, p. 109 878, 2024.

[27] C. Ansin, F. Larsson and R. Larsson, 'Fast simulation of 3d elastic response for wheel–rail contact loading using proper generalized decomposition,' *Computer Methods in Applied Mechanics and Engineering*, vol. 417, p. 116 466, 2023.

[28] W. Daves, W. Kubin, S. Scheriau and M. Pletz, 'A finite element model to simulate the physical mechanisms of wear and crack initiation in wheel/rail contact,' *Wear*, vol. 366-367, pp. 78–83, 2016.

[29] B. Andersson, M. Ekh and B. L. Josefson, 'Computationally efficient simulation methodology for railway repair welding: Cyclic plasticity, phase transformations and multi-phase homogenization,' *Journal of Thermal Stresses*, vol. 47, pp. 164–188, 2024.

[30] B. Andersson, 'Thermo-Mechanical-Metallurgical Modelling of Pearlitic Steels and Railhead Repair Welding (Doctoral thesis),' *Chalmers University of Technology*, 2024.

[31] C. Ansin, B. A. Pålsson, M. Ekh, F. Larsson and R. Larsson, 'Simulation and Field Measurements of the Long-Term Rail Surface Damage Due To Plasticity, Wear and Surface Rolling Contact Fatigue Cracks in a Curve,' *CM 2022 - 12th International Conference on Contact Mechanics and Wear of Rail/Wheel Systems, Conference Proceedings*, pp. 591–601, 2022.

[32] F. Sadeghi, B. Jalalahmadi, T. S. Slack, N. Raje and N. K. Arakere, 'A review of rolling contact fatigue,' *Journal of Tribology*, vol. 131, pp. 1–15, 2009.

[33] J. W. Ringsberg, 'Life prediction of rolling contact fatigue crack initiation,' *International Journal of Fatigue*, vol. 23, pp. 575–586, 2001.

[34] A. Kapoor, 'A re-evaluation of the life to rupture of ductile metals by cyclic plastic strain,' *Fatigue & Fracture of Engineering Materials & Structures*, vol. 17, pp. 201–219, 1994.

[35] K. Golos and F. Ellyin, 'A total strain energy density theory for cumulative fatigue damage,' *Journal of Pressure Vessel Technology, Transactions of the ASME*, vol. 110, pp. 36–41, 1988.

[36] F. J. Franklin, J. E. Garnham, D. I. Fletcher, C. L. Davis and A. Kapoor, 'Modelling rail steel microstructure and its effect on crack initiation,' *Wear*, vol. 265, pp. 1332–1341, 2008.

[37] G. Trummer, C. Marte, P. Dietmaier, C. Sommitsch and K. Six, 'Modeling surface rolling contact fatigue crack initiation taking severe plastic shear deformation into account,' *Wear*, vol. 352-353, pp. 136–145, 2016.

[38] M. Ghodrati, M. Ahmadian and R. Mirzaeifar, 'Modeling of rolling contact fatigue in rails at the microstructural level,' *Wear*, vol. 406-407, pp. 205–217, 2018.

[39] M. W. Brown and K. J. Miller, 'A Theory for Fatigue Failure under Multiaxial Stress-Strain Conditions,' *Proceedings of the Institution of Mechanical Engineers*, vol. 187, pp. 745–755, 1973.

[40] K. N. Smith, T. H. Topper and P. Watson, 'A stress-strain function for the fatigue of metals (stress-strain function for metal fatigue including mean stress effect),' *J Materials*, vol. 5, pp. 767–778, 1970.

[41] A. Ince and G. Glinka, 'A generalized fatigue damage parameter for multiaxial fatigue life prediction under proportional and non-proportional loadings,' *International Journal of Fatigue*, vol. 62, pp. 34–41, 2014.

[42] C. L. Pun, Q. Kan, P. J. Mutton, G. Kang and W. Yan, 'A single parameter to evaluate stress state in rail head for rolling contact fatigue analysis,' *Fatigue and Fracture of Engineering Materials and Structures*, vol. 37, pp. 909–919, 2014.

[43] Y. Jiang and H. Sehitoglu, 'A model for rolling contact failure,' *Wear*, vol. 224, pp. 38–49, 1999.

[44] N. Talebi, J. Ahlström, M. Ekh and K. A. Meyer, 'Crack Initiation Criteria for Deformed Anisotropic R260 Rail Steel,' *CM 2022 - 12th International Conference on Contact Mechanics and Wear of Rail/Wheel Systems, Conference Proceedings*, pp. 857–864, 2022.

[45] N. Talebi, J. Ahlström, M. Ekh and K. A. Meyer, 'Evaluations and enhancements of fatigue crack initiation criteria for steels subjected to large shear deformations,' *International Journal of Fatigue*, vol. 182, p. 108 227, 2024.

[46] D. Gren and J. Ahlström, 'Fatigue crack propagation on uniaxial loading of biaxially predeformed pearlitic rail steel,' *Metals*, vol. 13, p. 1726, 2023.

[47] J. A. Nelder and R. Mead, 'A Simplex Method for Function Minimization,' *The Computer Journal*, vol. 7, pp. 308–313, 1965.

[48] F. Gao and L. Han, 'Implementing the Nelder-Mead simplex algorithm with adaptive parameters,' *Computational Optimization and Applications*, vol. 51, pp. 259–277, 2012.

[49] M. J. Powell *et al.*, 'The BOBYQA algorithm for bound constrained optimization without derivatives,' *Cambridge NA Report NA2009/06, University of Cambridge, Cambridge*, vol. 26, pp. 26–46, 2009.

[50] N. Andréasson, A. Evgrafov, M. Patriksson *et al.*, 'An introduction to continuous optimization, 3rd edition,' *Studentlitteratur*, 2016.

[51] M. Ekh, A. Johansson, H. Thorberntsson and B. L. Josefson, 'Models for cyclic ratchetting plasticity—integration and calibration,' *J. Eng. Mater. Technol.*, vol. 122, pp. 49–55, 2000.

[52] K. A. Meyer, 'Evaluation of material models describing the evolution of plastic anisotropy in pearlitic steel,' *International Journal of Solids and Structures*, vol. 200, pp. 266–285, 2020.

[53] D. Hérault, S. Thuillier, S. Y. Lee, P. Y. Manach and F. Barlat, 'Calibration of a strain path change model for a dual phase steel,' *International Journal of Mechanical Sciences*, vol. 194, 2021.

[54] M. Stone, 'Cross-Validatory Choice and Assessment of Statistical Predictions,' *Journal of the Royal Statistical Society*, vol. 36, pp. 111–147, 1974.